Journal of Inflammation Research

Dovepress
Taylor & Francis Group

Open Access Full Text Article

ORIGINAL RESEARCH

Rat Model of Granulomatous Mastitis

Jie Gong[1,2], Juan Wang[1,2], Xin Zhong[1,2], Yao Zhou[1,2], Lele Shen[1,2], Xianguang Deng[1], Anqi Ge[1], Lifang Liu[1]

[1]Department of Galactophore, The First Affiliated Hospital of Hunan University of Chinese Medicine, Changsha, Hunan, 410007, People's Republic of China; [2]Graduate School of Hunan University of Chinese Medicine, Changsha, Hunan, 410208, People's Republic of China

Correspondence: Anqi Ge; Lifang Liu, Email ge_anqi@126.com; lifang_liu@hnucm.edu.cn

Background: Granulomatous mastitis (GM) is an immune-related, clinically refractory disease, the translational research of which has been hindered by the lack of animal models. Establishing a stable rat model of GM is critical for elucidating its mechanisms and developing therapeutic approaches.

Methods: The first batch of rats was randomly divided into a normal group, a low-dose group (0.2 mL), a middle-dose group (0.4 mL), and a high-dose group (0.8 mL). Except for the normal group, the remaining groups were subjected to model establishment using a tissue homogenate-complete Freund's adjuvant (CFA) suspension. The optimal dose was determined based on gross morphology, mammary inflammation index, and histopathological evaluation. The second batch of rats was modeled using the optimal dose, with a comparable number of normal rats as controls. At 7, 14, 21, and 28 days post-modeling, mammary gland appearance, histomorphology, and serum/tissue mRNA expression levels of key inflammatory factors (TNF-α, IL-1β, IFN-γ, IL-2) were observed.

Results: Rats in the middle-dose group exhibited characteristic features of human GM, including gross morphological changes such as breast swelling, ulceration, and fistula formation. Histologically, granulomas characterized by epithelioid cells and Langhans multinucleated giant cells, along with persistent inflammatory cell infiltration, were observed. Compared with the parallel normal group, the expression levels of IL-2, IL-1β, TNF-α, and IFN-γ were significantly elevated in the model group, with their expression fluctuating over time.

Conclusion: The 0.4 mL tissue homogenate-CFA injection method successfully induced a stable, reproducible, and long-lasting rat model that closely mimics human GM. This model provides a robust foundational platform for future research.

Keywords: granulomatous mastitis, tissue homogenate-CFA injection method, animal model, autoimmunity

Introduction

Granulomatous mastitis (GM), a nonspecific chronic inflammatory breast disease with an uncertain etiology, occurs primarily during non-lactation periods. First described by Kessler and Wolloch in 1972,[1] GM is also known as granulomatous lobular mastitis (GLM) because its lesions are centered on the breast's terminal ductal lobular units. Clinically, the disease manifests as the sudden appearance of breast lumps or abscesses, which may progress to skin ulceration, sinus formation, and fistulas. GM is known for its protracted course and high recurrence rate. Over the past two decades, the incidence of GM has escalated rapidly, now accounting for 24% of all inflammatory breast disease cases, making it a widely reported breast condition internationally.[2,3] Current treatment options mainly consist of glucocorticoids, broad-spectrum antibiotics, immunosuppressants, and surgical intervention. However, treatment efficacy varies among individuals, and recurrence rates remain high. Although traditional Chinese medicine has demonstrated clinical benefits in symptom improvement and recurrence control, its molecular mechanism remains to be systematically investigated.[4] The absence of a standardized treatment approach contributes to the poor clinical efficacy of GM, sometimes colloquially referred to as the "cancer that won't die."

However, the pathophysiology of this disease has not been fully elucidated, and there are no specific diagnostic markers. It is generally believed that it may be associated with various factors such as α1-antitrypsin deficiency, hyperprolactinemia,[5] use of oral contraceptives,[6] smoking, and trauma-induced factors. Some scholars believe that

Received: 28 April 2025
Accepted: 15 July 2025
Published: 17 July 2025

Corynebacterium, especially *Corynebacterium parakroppenstedtii (C. parakroppenstedtii)* and *Corynebacterium kroppenstedtii (CK)* infections, may be closely related to the occurrence of this disease, and related research is becoming a new hot spot.[7,8] In recent years, GM has been more inclined to be studied as an autoimmune disease, and autoimmune abnormalities may play a key role in its pathophysiology. For instance, patients with GM frequently exhibit activated humoral immune function, as evidenced by significantly elevated levels of C3, C4, IgE, and IgA.[9] Additionally, tissue IgG4 levels have been implicated in influencing both the therapeutic efficacy of glucocorticoid treatment and the risk of disease recurrence.[10] Studies have shown that dysfunction of T cells, B cells, and natural killer (NK) cells, as well as the excessive release of inflammatory cytokines such as interleukin-2 (IL-2), interleukin-1β (IL-1β), tumor necrosis factor-α (TNF-α) and interferon-γ (IFN-γ), are important factors driving the development of GM.[11] Therefore, more basic research is needed to answer the above questions.

Although there have been numerous case reports and clinical retrospective studies on GM, related basic research is relatively scarce. This is largely related to the lack of mature animal models. So far, there is no unified standard animal modeling method, and fewer than 10 articles specifically dedicated to GM animal model research can be retrieved. These studies have reflected the disease characteristics of GM to some extent, but there is still room for further optimization in terms of histological features, inflammatory response intensity, and model stability to better simulate the clinical and pathological features of human GM.

After a comprehensive analysis of existing modeling methods, we decided to establish a rat GM model using a combination of human breast tissue homogenate and complete Freund's adjuvant (CFA) subcutaneous injection. The model has been systematically evaluated in terms of histopathological changes, inflammation level, and key immune factor expression. The goal is to construct a reproducible, stable animal model with pathological features closer to human GM, providing a reliable experimental basis for subsequent mechanistic studies and the development of treatment strategies.

Materials and Methods

Animals

A total of 72 SPF-grade female SD rats (6–7 weeks old, weighing 200±20 g) were provided by Hunan Slaike Jingda Laboratory Animal Co., Ltd. [Changsha, China; Certificate No. SCXK(Xiang)2019–0004]. All study animals were maintained under standard atmospheric pressure, a 12/12-hour light/dark cycle, room temperature of 22±1°C, and relative humidity of 50±5%. They were randomly housed in cages with free access to water and food, and the experiment began after 7 days of adaptive feeding. The experimental design and procedures strictly followed the standards established by the Experimental Animal Ethics Committee of the First Affiliated Hospital of Hunan University of Chinese Medicine, complying with relevant regulations on experimental animal welfare and ethics (Hunan, China; Ethical Approval No. 202404015).

Reagents and Instruments

CFA (Sigma-Aldrich, USA); Enzyme-Linked Immunosorbent Assay (ELISA) kits for IL-2, IL-1β, TNF-α, IFN-γ (Elabscience, Wuhan, China); Low-temperature tissue grinder (JXFSTPRP-CL, Shanghai Jingxin Industrial Development Co., Ltd., China); Fully automated digital pathology scanner (Pannoramic MIDI, 3DHISTECH, Hungary); Multi-function enzyme labeling instrument (Varioskan Flash, Thermo Fisher Scientific, USA); Ultrasonic machine (VINNO 6 LAB, Feiyino Technology Co., Ltd., Suzhou, China).

Homogenate Preparation

Lesion tissues from GM patients (including firm granuloma-containing breast tissue or necrotic tissue) were aseptically excised using a cold knife during surgery and preserved in sterile 0.9% normal saline (NS) at 4°C.The fresh GM tissues were pretreated by rinsing with 0.9% NS to remove excess blood and pus. The GM tissues were placed in grinding tubes, added with an equal volume of NS, and 3 small grinding beads and 1 large grinding bead. The low-temperature tissue grinder was set to a temperature of −50°C and a vibration frequency of 50 Hz. Each grinding session lasted for

30 seconds with a 10-second interval, repeated 5–8 times until the tissues were fully pulverized. Finally, the prepared homogenate was mixed with CFA at a 1:1 ratio to create an oil-in-water emulsion suspension, which was stored at 4°C for future use.The diseased tissues used in this study were obtained from four clinically and pathologically confirmed GM patients aged 25–45 years, who were non-pregnant, non-lactating, and without concurrent inflammatory conditions or autoimmune diseases. The study protocol was approved by the Ethics Committee of the First Affiliated Hospital of Hunan University of Chinese Medicine (Approval number: HN-LL-KY-2021-020-01), and written informed consent was obtained from all donors. The experiments were conducted in accordance with the Declaration of Helsinki.

Rat Model Establishment and Experimental Design

The experiment was divided into two parts. The first part aimed to determine the optimal injection dose for modeling, while the second part aimed to observe changes in the model rats.

In the first part, normal, low-dose, middle-dose, and high-dose groups were designed. Twenty-four rats were randomly divided into these four groups, with six rats in each group. Except for the normal group, all other rats underwent model establishment. The rats were anesthetized using 5% pentobarbital sodium (45 mg/kg, intraperitoneal injection) and exposed by shaving. Using a 1 mL syringe (with a 2.5 mL syringe needle), 0.2 mL, 0.4 mL, and 0.8 mL of the oil-in-water emulsion suspension were injected into the subcutaneous mammary fat pad of the left third mammary gland of rats in the low-dose, middle-dose, and high-dose groups, respectively. After injection, the needle was slowly rotated and withdrawn, and a gauze or cotton ball was used to press the needle hole to reduce leakage of the emulsion suspension. The condition of the implanted mammary gland site was observed on days 3, 7, and 14 after modeling, and the body weight of the rats was measured. After 14 days of routine maintenance feeding, the left third mammary gland tissues of the rats in each group were collected under anesthesia and stored in 4% paraformaldehyde solution until histopathological examination. At the end of the experiment, all animals were euthanized by overdose injection of pentobarbital sodium (150 mg/kg, intraperitoneal injection).

In the second part, normal and model groups were designed. Forty-eight rats were randomly divided into these two groups, with twenty-four rats in each group. All rats in the model group underwent model establishment. After anesthetizing the rats and exposing them by shaving, the optimal dose (determined from the first part of the experiment) of the oil-in-water emulsion suspension was injected into the subcutaneous mammary fat pad of the left third mammary gland for injection embedding. Changes in the condition of the rats in each group were observed after modeling. Body weight measurements and tissue collections were performed on days 7, 14, 21, and 28 after modeling, with six rats randomly selected from each group at each time point. After anesthesia, blood was collected and serum was separated, and mammary gland tissues were also collected for subsequent analysis. At the end of the experiment, all animals were euthanized.

Assessment of Breast Inflammation Index (BII) in Rats

The local manifestations of the mammary glands in each group of rats were observed for signs of increased overall body temperature and/or local mammary gland skin temperature. The presence of breast lumps, redness, pus discharge, fistulas, as well as behavioral changes such as sluggishness and lethargy were noted. Monitor for the appearance or improvement of these symptoms, and assign scores based on the symptomatic manifestations observed in each group of rats. The final inflammation index will be calculated as the sum of all individual scores, with specific scoring criteria outlined in Table 1[12]

Histopathological Evaluation

The mammary gland tissue from the third left breast of the rats was fixed in 4% paraformaldehyde, subsequently embedded in paraffin, and sectioned at 4 μm. The tissue sections were then dewaxed using xylene solution and stained with hematoxylin and eosin (H&E). The morphological features of the mammary tissue were observed under a microscope, and the tissue sections were scanned using an automatic digital pathology scanner. Image analysis was performed using the accompanying software, SlideViewer 2.6. The successful establishment of the animal model was determined based on the pathological features of GM, primarily including granuloma formation centered around

Table 1 BII Score of Rats

Scoring/Points	Symptoms
0	Normal mammary glands, no redness or swelling
1	Poor mental state and sluggish movement in rats
1	Redness of the skin on or around the mammary glands of rats, or visible lumps
1	Reactions such as foot withdrawal, struggling, or squealing when pressing on or around the mammary glands of rats
1	Higher skin temperature on the surface of the mammary glands compared to the normal group
3	Rupture and pus discharge visible on or around the surface of the mammary glands

Notes: A total score of 1–2 indicates mild inflammation of the mammary glands in rats, while a score of 3 or above indicates significant inflammation.

mammary lobules, inflammatory cell infiltration, duct and lobule destruction, microabscess formation, fat necrosis, and lipid vacuoles.

Analysis of Serum Inflammatory Factors by ELISA

After bringing the serum to room temperature, it was centrifuged at 1000 rpm and 4°C for 20 minutes, and the supernatant was used for ELISA detection. ELISA kits were used to detect the levels of IL-2, IL-1β, TNF-α, and IFN-γ in the serum according to the manufacturer's instructions. The OD values were measured at 450 nm using a microplate reader.

Analysis of Tissue Inflammatory Genes by qRT-PCR

Quantitative real-time polymerase chain reaction (qRT-PCR) was performed to quantitatively analyze the relative gene expression of IL-2, IL-1β, TNF-α, and IFN-γ in mammary tissue. Following the manufacturer's instructions, approximately 50 mg of tissue samples were taken, ground in liquid nitrogen, and total RNA was extracted using RNAiso Plus (TAKARA, 9109). After chloroform layering, RNA was precipitated with isopropanol, washed with 75% ethanol, and finally dissolved in DEPC water. The RNA concentration was determined using a micro-spectrophotometer (Micro Drop, Shanghai Baoyude Scientific Instrument Co., Ltd., China). Subsequently, RNA was reverse transcribed into complementary deoxyribonucleic acid (cDNA) using the PrimeScript™ RT kit (TAKARA, RR037A). qRT-PCR was performed using the ViiA7 Real-Time PCR System (ABI, USA) and HieffTM qPCR SYBR Green Master Mix (YEASEN, China). The GAPDH gene was used as a reference for normalizing the experimental data, and all results were calculated using the 2-ΔΔCt method. The primer sequences (5'-3') are as follows: IL2 forward: TTTGAGTGCCAATTCGATGA, reverse: TGATGCTTTGACAGATGGCTA; IL-1β forward: CCTATGTCTTGCCCGTGGAG, reverse: CACACACTAGCAGGTCGTCA; TNF-α forward: GCTCCCTC TCATCAGTTCCA, reverse: GCTTGGTGGTTTGCTACGAC; INF-γ forward: GGCAAAAGGACGGTAACACG, reverse: TTCACCTCGAACTTGGCGAT; GAPDH forward: AGACAGCCGCATCTTCTTGT, reverse: TGATGGCAACAATGT CCACT.

Small Animal B-Mode Ultrasonography

The chest hair of rats in each group was shaved cleanly, and they were fixed in a supine position. After evenly applying coupling agent to the examination site, a small animal B-mode ultrasonography machine equipped with an X6-16L (18 MHz frequency) probe was used to examine the breast conditions of the rats in each group.

Statistical Analysis

Experimental data were analyzed and visualized using GraphPad Prism 10.1.2. Differences among multiple groups were evaluated by one-way analysis of variance (ANOVA) or the Kruskal–Wallis test. Pairwise comparisons between groups were performed using Tukey's HSD or Dunn's test, with significance adjusted by Bonferroni correction. Data are described as mean ± standard deviation or median (interquartile range), with significance marked as $*P < 0.05$ and $**P < 0.01$.

Results

The Optimal Injection Volume for Modeling Was Determined to Be 0.4mL

General Evaluation of Rats in Different Groups

During the experiment, two rats in the high-dose group died, one on the 8th day and the other on the 12th day after modeling. At the end of the experiment, rats in the normal group appeared to be in good general condition with normal physical appearance. Rats in the low-dose and middle-dose groups showed increased activity and struggling behavior, while rats in the high-dose group exhibited reduced activity, lethargy, increased struggling when handled, and irritability.

The body weight of rats in all groups showed an increasing trend over time. There were no significant differences in body weight between the low, medium, and high-dose groups compared to the parallel normal group at 3 and 7 days after modeling ($P > 0.05$). However, at 14 days, the body weight of the high-dose group was significantly lower than that of the parallel normal group ($P < 0.05$) (Figure 1). This suggests that an injection volume of 0.8mL for modeling results in slower body weight gain in rats, and that injecting a large volume of homogenate may have a negative impact on the physiological state of the rats, possibly contributing to the death events.

Assessment of Rat Mammary Gland Appearance and BII

The mammary glands of rats in the normal group appeared healthy, whereas those in the low, medium, and high-dose model groups exhibited varying degrees of inflammatory changes. After 14 days of modeling, the breast lumps in the low-dose group decreased in size, indicating a trend of inflammation subsiding. In the middle-dose group, visible lumps and even ulcerations were observed. In the high-dose group, the rats developed large breast lumps accompanied by severe redness, ulceration, and purulent discharge (Figure 2).

On days 3, 7, and 14 after modeling, the mammary inflammation index scores of rats in the medium and high-dose groups were significantly higher than those in the parallel normal group ($P < 0.01$) (Table 2). Although the scores in the low-dose group were elevated compared to the normal group, the difference was not statistically significant ($P > 0.05$).

Pathological Changes

The histopathological characteristics of the third mammary gland tissue on the left side of rats in each group are shown in Figure 3. Normal group: Normal mammary glands with clear acini and stroma were observed. Low-dose group: The granuloma structure was not prominent, and the lobular structure of the mammary gland was still distinct. There was infiltration of plasma cells, neutrophils, and other inflammatory cells, with scattered lipid droplet vacuoles of varying sizes. Middle-dose group: Prominent granuloma structures were visible, distributed in a multi-nodular pattern, disrupting the lobular structure. The granulomas consisted of epithelioid cells and Langhans-type multinucleated giant cells. Large lipid droplet vacuoles were observed in the center of the granulomas, surrounded by a significant gathering of

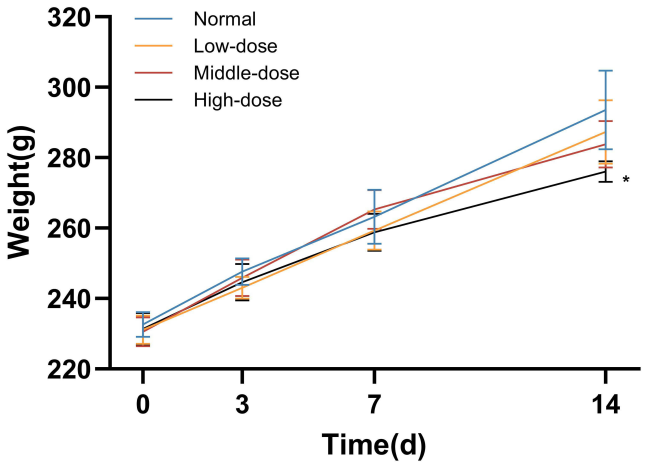

Figure 1 Changes in body mass of rats in different groups on the day of modeling (0 days), and 3, 7, and 14 days after modeling. Values at 0, 3, and 7 days represent mean ± standard deviation, while the value at 14 days is the median *$P < 0.05$ compared to the parallel normal group.

https://doi.org/10.2147/JIR.S537209

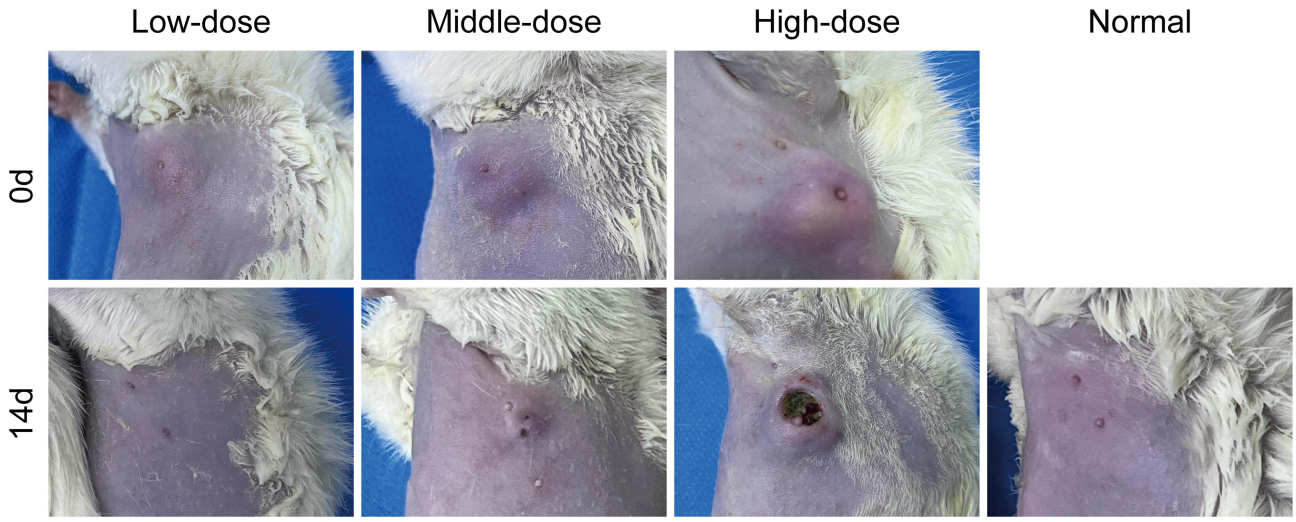

Figure 2 Mammary gland appearance of rats in each group 14 days after modeling. The size of breast lumps and the degree of local inflammation followed the order: high-dose group > middle-dose group > low-dose group. The lumps in the low-dose group subsided the fastest, and the mammary gland appearance was almost indistinguishable from the normal group 14 days after modeling. The high-dose group showed the most destructive lumps, with large areas of skin ulceration and purulent discharge.

neutrophils. Notable lymphocytes and plasma cells, along with a few eosinophils, were present. Microabscess formation was also observed. High-dose group: A heavy inflammatory background was noted, but without distinct granulomatous nodules. Severe disruption of mammary lobules and ductal structures was observed, accompanied by fat necrosis and large lipid vacuoles.

Based on the above findings, we conclude that the middle-dose group (0.4mL) yields the best modeling effect. Rats in this group exhibited typical inflammatory appearance and elevated mammary inflammation index. HE staining revealed distinct granuloma structures composed of epithelioid cells and Langerhans multinucleated giant cells. Histopathology currently stands as the "gold standard" for diagnosing this disease. In contrast, the low-dose group (0.2mL) showed relatively mild inflammation, and the granuloma structure was not pronounced. The morphological features of inflammatory cell infiltration and lipid droplet vacuole distribution were not sufficient to support the simulation of GM. Additionally, the short duration of the model's maintenance was not conducive to basic research. Although the BII of the high-dose group (0.8mL) was elevated compared to the normal group and showed no significant difference from the medium-dose group, its pathological manifestations were less characteristic than the latter. It appeared more like a result of severe inflammation leading to extensive necrosis of local tissue. Most importantly, the large lumps and skin ulcerations caused significant pain to the experimental animals. Animal growth was noticeably inhibited at this dose, and we suspect that over time, animals may develop other unpredictable complications or even death due to the burden of the model. Adhering to the 3R principles of animal experimentation (Replace, Reduce, and Refine),[13] we aim to achieve ideal modeling results while minimizing animal suffering. Therefore, we have decided to use the moderate dose as the modeling dose for subsequent experiments.

Table 2 BII Scores in Each Group [M(P25,P75)]

Group	Injection dose/mL	3d	7d	14d
Normal	0	0.00 (0.00,0.00)	0.00 (0.00,0.00)	0.00 (0.00,0.00)
Low-dose	0.2	1.00 (1.00,2.25)	2.00 (1.00,3.25)	2.50 (1.75,3.50)
Middle-dose	0.4	3.00 (2.75,4.50)**	6.00 (5.00,6.00)**	6.00 (5.75,6.25)**
High-dose	0.8	3.50 (3.00,6.00)**	6.00 (5.75,6.00)**	6.50 (6.00,7.00)**

Note: **$P < 0.01$ vs parallel normal group.

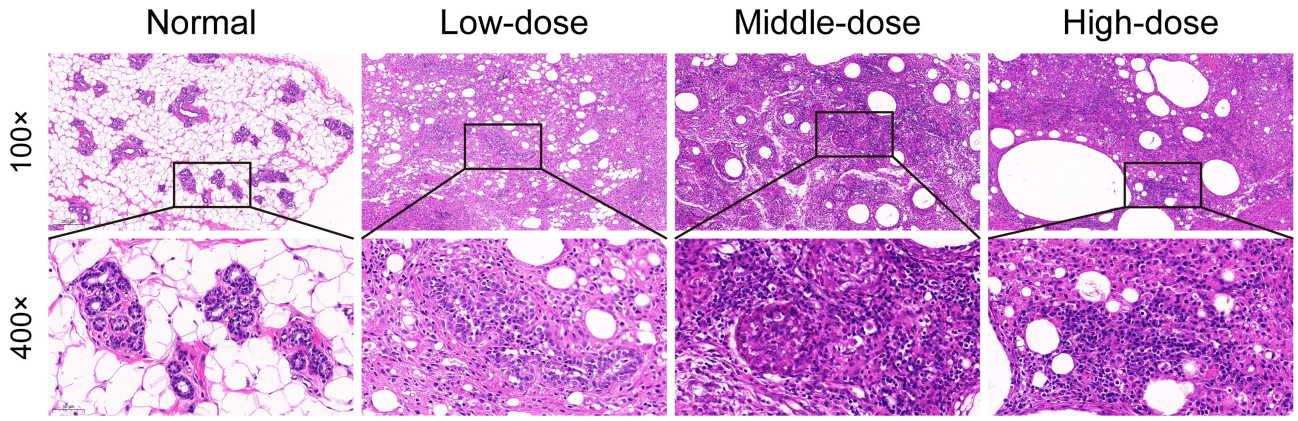

Figure 3 Effects of different doses of oil-in-emulsion suspension on histopathological changes in rat mammary gland tissue 14 days after modeling. HE staining. Upper images: Magnification = 100× (scale bar = 200um); Lower images: Magnification = 400× (scale bar = 50um).

Disease Progression and Changes of Inflammatory Factor Expression in GM Model Rats

Symptoms and Weight Changes

During the experiment, rats in the normal group appeared normal in appearance and behavior, with agile bodies, shiny hair, and normal stool. Rats in the model group showed increased activity, struggling, and fighting behavior in the early stage of modeling (0~14d), while in the later stage (14~28d), they exhibited disheveled hair, reduced food intake and activity, and a leaner body type.

The weight of rats in the normal group showed a steady increase. In the model group, rat weight increased stably in the early stage of modeling but grew slowly and was lighter compared to the normal group in the later stage. On days 21 and 28 after modeling, the weight of rats in the model group was significantly lower than that in the normal group ($P < 0.01$) (Figure 4).

Changes in Breast Appearance and Assessment of Inflammation

The mammary glands of rats in the normal group appeared normal. However, in the model group, the mammary glands exhibited a basic trend of changes from redness and swelling to ulceration and pus discharge, followed by a reduction in the size of the mass. Specifically, at 7 days after modeling, obvious masses were visible in the rats' mammary glands, with bright red skin color and even local heat; at 14 days, the masses ulcerated and discharged pus; at 21 days, the ulcerated areas gradually healed and dried up, and the masses became smaller than before, forming sinuses or fistulas; at 28 days, the masses were significantly reduced or even disappeared, and pigmentation was visible at the lesion sites

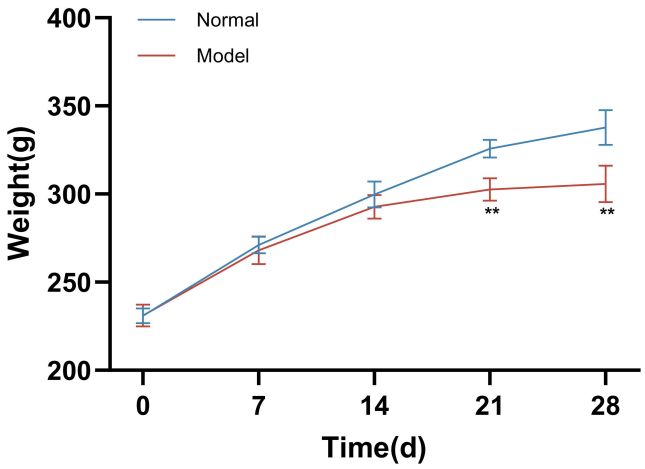

Figure 4 Changes in body weight of rats in the normal and model groups over time. Values are mean ± standard deviation. **$P < 0.01$ vs the parallel normal group.

https://doi.org/10.2147/JIR.S537209

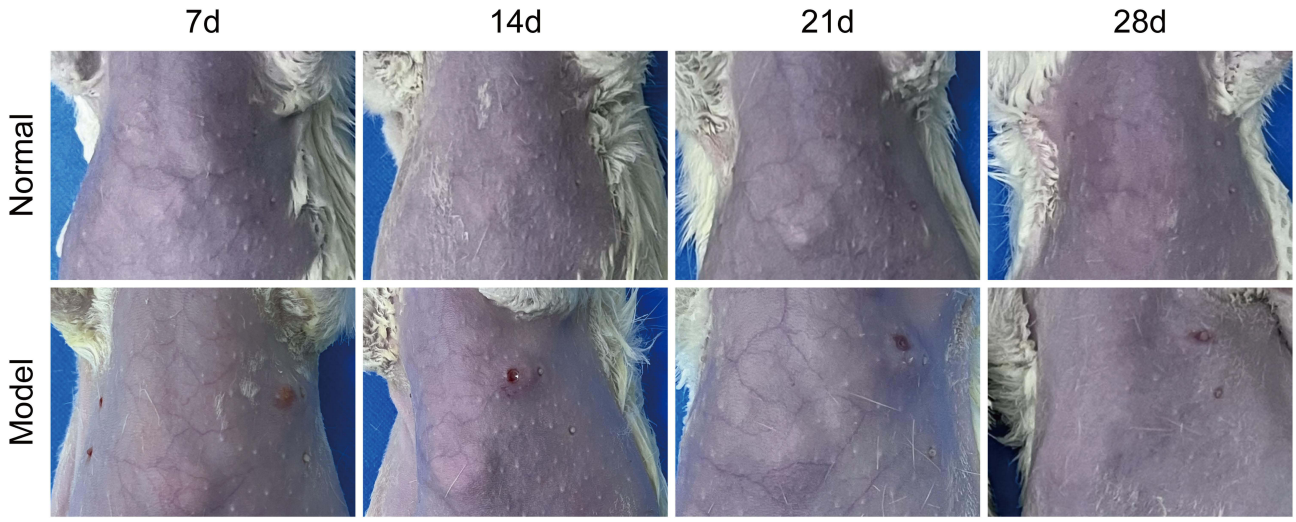

Figure 5 Appearance of the mammary glands in the model group at 7, 14, 21, and 28 days after modeling.

(Figure 5). Compared to 7 and 14 days after modeling, the breast inflammation index score of the model group was significantly lower at 28 days after modeling ($P < 0.01$) (Table 3).Small animal B-ultrasound showed no abnormalities in the mammary glands of the normal group. In the model group, the lesion morphology and echo characteristics gradually changed over time at different time points (days 7, 14, 21, and 28). Specifically, at 7 days after modeling, there were obvious lesions (masses and internal abscess cavities) in the rats' mammary glands; at 14 days, the abscess cavity expanded; at 21 days, the abscess cavity shrank; and at 28 days, the lesion boundaries were blurred, and the abscess cavity was significantly reduced (Figure 6). These findings suggest that this GM rat model may be a self-limiting model, which can disappear or exhibit insignificant features over time.

Pathological Changes

Histopathological examination revealed that the breast structure of rats in the normal group remained clear and normal at all time points. In the model group, after 7 days of modeling, distinct granuloma structures were observed, along with numerous multinucleated giant cells and neutrophils. The breast lobule tissue structure was disrupted, surrounded by lymphocytes, plasma cells, monocytes, and other inflammatory cells. At 14 days of modeling, a prominent granulomatous ring structure composed of epithelioid cells was visible. The breast lobule structure was deformed, with epithelial lining shedding and infiltration of a large number of inflammatory cells, including plasma cells. By 21 days of modeling, there was extensive infiltration of inflammatory cells around the granulomas, destruction of mammary ducts, shedding of epithelial lining, and the formation of a few small blood vessels. At 28 days of modeling, a small amount of granuloma structures were observed around the acini, accompanied by duct dilation, fibrosis, and numerous scattered small lipid droplet vacuoles (Figure 7). Thus, it can be inferred that as time progressed, the inflammatory pathological changes in the model group rats gradually subsided, and the granuloma structures decreased. The formation of small blood vessels and duct fibrosis observed in the later stages of modeling suggest possible tissue self-repair in the rat mammary glands.

Table 3 BII Scores in the Normal Group and Model Group [M(P25, P75)]

Group	7d	14d	21d	28d
Normal	0.00 (0.00,0.00)	0.00 (0.00,0.00)	0.00 (0.00,0.00)	0.00 (0.00,0.00)
Model	6.00 (5.75,6.00)**	6.00 (5.00,7.00)**	5.00 (4.50,6.25)	2.00 (1.75,3.00)

Note: **$P < 0.01$ vs model group at 28 days.

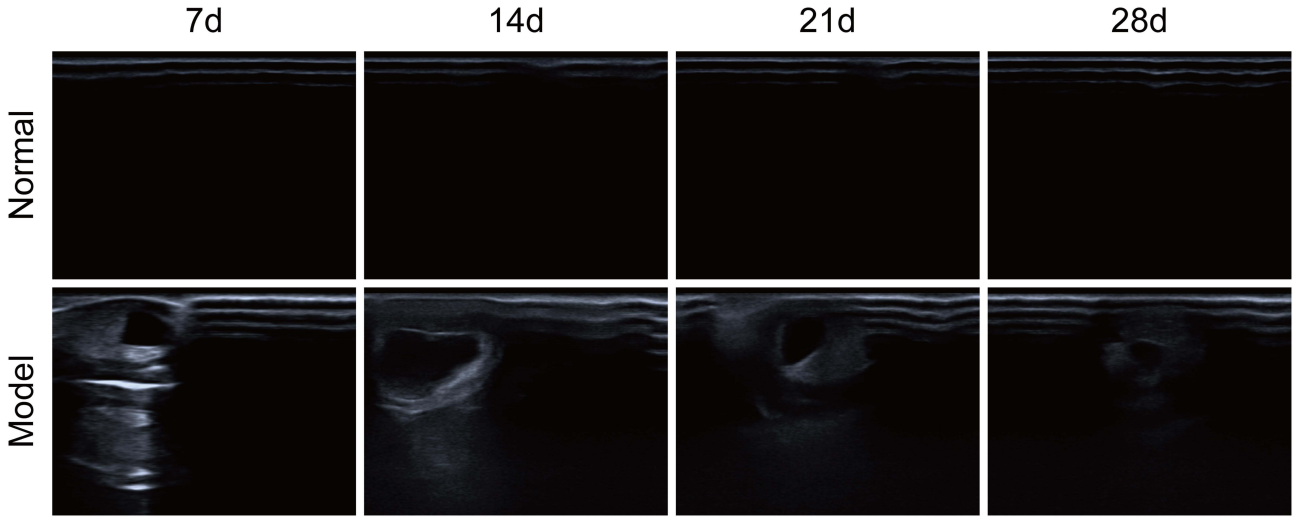

Figure 6 B-ultrasound morphology of the mammary glands in the model group at 7, 14, 21, and 28 days after modeling. At 7 days after modeling, obvious irregular hypoechoic areas were visible, with anechoic areas inside, and strong echo bands with posterior acoustic shadowing or attenuation were visible below; at 14 days, the hypoechoic areas shrank, and the internal anechoic dark fluid areas expanded; at 21 days, both the hypoechoic and anechoic areas shrank; at 28 days, the hypoechoic areas were significantly reduced with blurred boundaries, and a small amount of residual anechoic areas were visible.

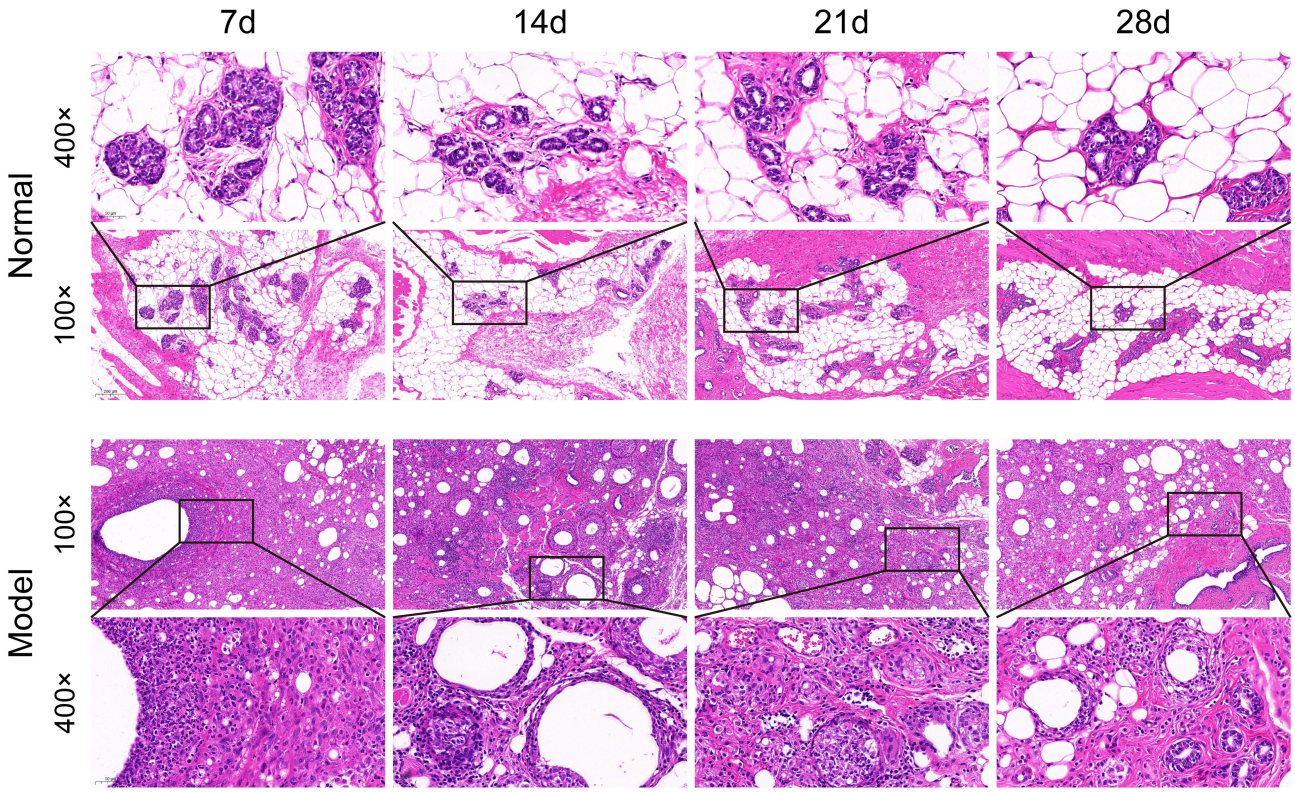

Figure 7 Histopathological changes in breast tissue of rats in the model group at 7, 14, 21, and 28 days after injection with 0.4mL of oil-in-emulsion suspension. HE staining. Magnification = 100× (scale bar = 200um); Magnification = 400× (scale bar = 50um).

Elisa

The levels of inflammatory cytokines IL-2, IL-1β, TNF-α, and IFN-γ in the serum of rats from both the normal and model groups were determined over time. Compared to the parallel normal group, the levels of these serum inflammatory factors were significantly elevated in the model group ($P < 0.01$). When compared to day 7 of modeling, the levels of IL-2 and IL-1β

https://doi.org/10.2147/JIR.S537209

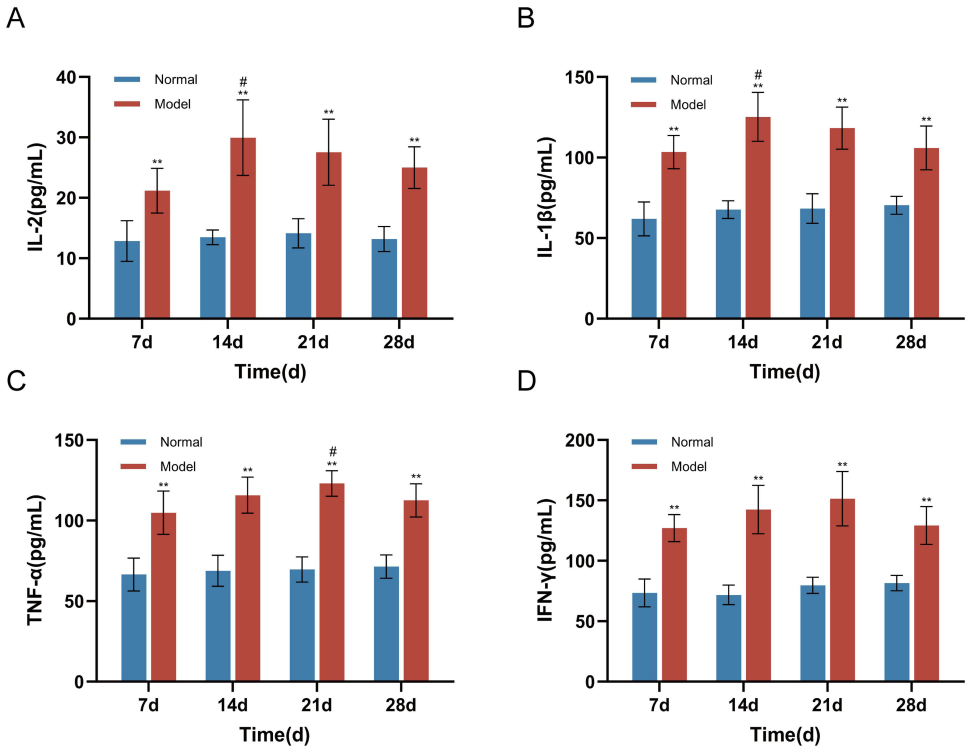

Figure 8 Changes in serum inflammatory factor expression in rats of each group. (**A**): IL-2 expression, (**B**) IL-1β expression, (**C**) TNF-α expression, (**D**) IFN-γ expression. $^{**}P < 0.01$ vs parallel normal group; $^{\#}P < 0.05$ vs 7d in this group.

increased at day 14 ($P < 0.05$), while the level of TNF-α rose at day 21 ($P < 0.05$) in the model group. Additionally, there were no differences in the levels of these serum inflammatory factors at different time points in the normal group ($P < 0.05$) (Figure 8).

qRT-PCR

The relative expression levels of IL-2, IL-1β, TNF-α, and IFN-γ mRNA in mammary gland tissues of rats in the normal and model groups were determined over time. The model group exhibited a persistent inflammatory response during the experiment. Compared to the parallel normal group, the relative mRNA expression of these cytokines was significantly increased in the model group ($P < 0.01$). When compared to day 7 of modeling, the expression of IL-2 increased at day 14 ($P < 0.05$), while the expressions of IL-1β, TNF-α, and IFN-γ were significantly elevated at days 14 and 21 ($P < 0.01$, $P < 0.05$) in the model group. Additionally, TNF-α remained highly expressed at day 28 of modeling ($P < 0.05$). Furthermore, compared to day 7 in the same group, the expressions of IL-1β and TNF-α increased at days 21 and 28 in the normal group ($P < 0.01$, $P < 0.05$), but these levels were much lower than those in the model group ($P < 0.01$) (Figure 9). This may suggest physiological inflammation regulation in rats due to hormonal changes or minor environmental stress.

Discussion

In previous studies, the available methods for establishing GM animal models can be summarized as human breast tissue homogenate combined with complete Freund's adjuvant injection, metoclopramide-induced prolactin elevation combined with human milk injection, and bacterial infection. For instance, Zuo et al[14] induced rat mammary glands to develop symptoms such as redness, swelling, and difficulty in healing after rupture by injecting a suspension of human GM tissue homogenate mixed with complete Freund's adjuvant. HE staining of breast tissue revealed pathological changes similar to human GM, including blurred boundaries of mammary lobules, accumulation of neutrophils and macrophages, dilation of mammary ducts, and vacuoles within the lobules. This was an early experimental study on GM animal models.

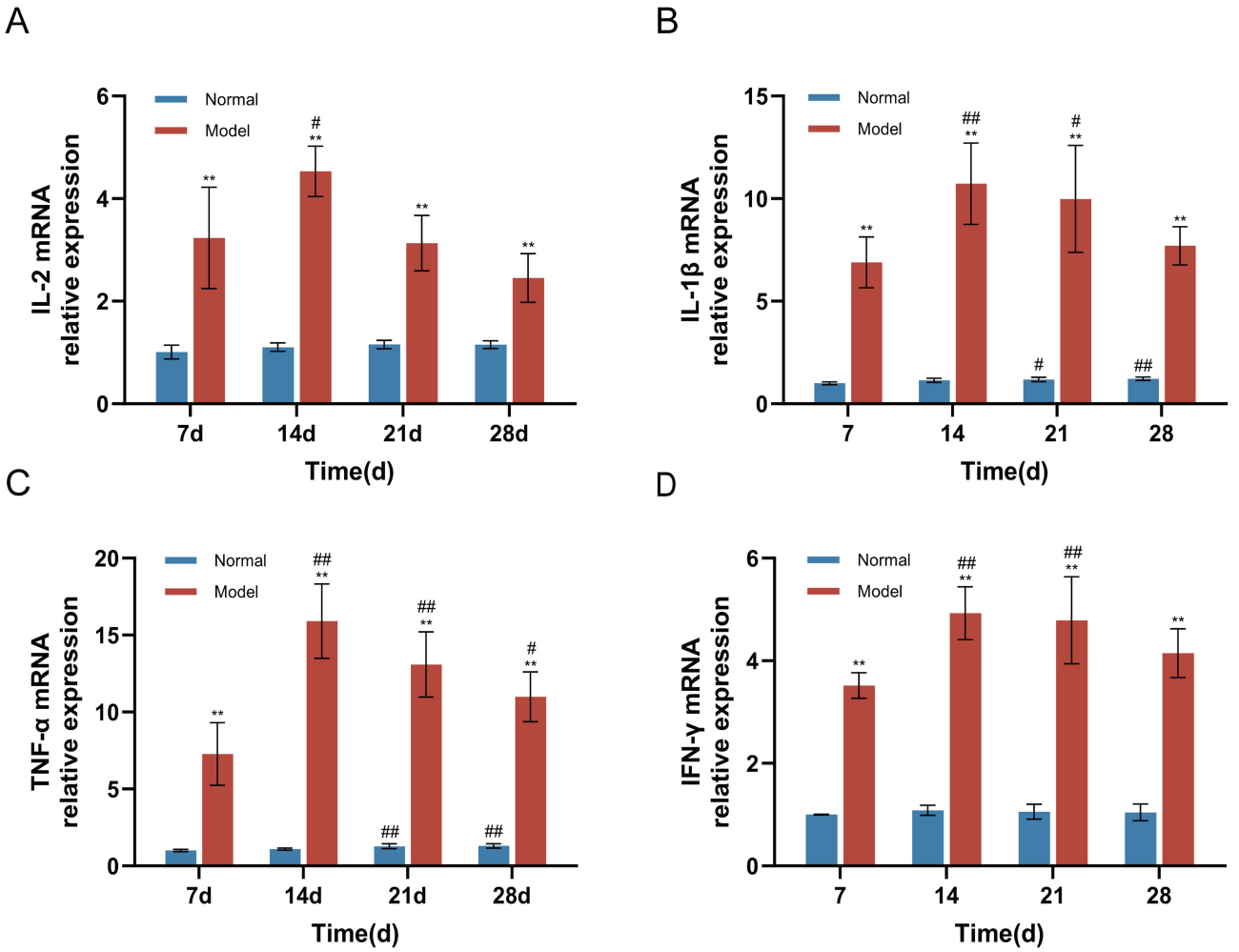

Figure 9 Changes in mRNA expression of inflammatory genes in rat mammary tissue in each group. (**A**): IL-2 expression, (**B**) IL-1β expression, (**C**) TNF-α expression, (**D**) IFN-γ expression. $^{**}P < 0.01$ vs parallel normal group; $^{\#}P < 0.05$ vs 7d in this group; $^{\#\#}P < 0.01$ vs 7d in this group.

Additionally, some scholars have utilized different substances to simulate the inflammatory appearance and pathological changes of clinical human GM patients by injecting them into animal breasts, based on possible etiologies of GM. For example, Ma et al[15] established an endocrine-related GM rat model by inducing a hyperprolactinemia state through subcutaneous injection of metoclopramide into the back and injecting human milk plus adjuvant suspension. The model rats developed breast masses with ulceration, elevated serum levels of PRL, IL-6, and IL-1β, and pathological manifestations such as granulomatous nodules and infiltration of various inflammatory cells. Liu et al[16] used human GM tissue homogenate plus CFA injection to establish a rat model under a hyperprolactinemia background, and further validated the model's dependency on a complete immune system through the failure of modeling in nude rats. This provided evidence for exploring the immune mechanism of GM. In recent years, the bacterial infection mechanism has received more attention. Liu et al[7] identified and isolated C. parakroppenstedtii, which was confirmed in vivo to induce GM-like lesions alone. They discovered a novel glycolipid secreted by this bacterium (called corynekropbactins), which acts as a pathogenic factor with iron chelation, cytotoxicity, and inflammatory factor-inducing effects. Recently, Zhang et al[17] constructed a cystic neutrophilic granulomatous mastitis (CNGM) model induced by a combination of lesion tissue and CK suspension injection, representing an infection-related GM model. The model rats exhibited breast redness and swelling, with typical features such as lipid vacuoles and Gram-positive bacilli visible under the microscope. However, GM is actually a disease with complex etiologies, promoted by multiple factors. Patients often have autoimmune dysfunction and elevated serum prolactin simultaneously, and specific pathogens are detected. Alternatively, a small

https://doi.org/10.2147/JIR.S537209

number of patients still lack a clear etiology despite comprehensive testing and clinical analysis.[18] Modeling based on a single etiology makes it difficult for the model to have broad representativeness and applicability. Furthermore, these modeling methods have not yet met the ideal experimental requirements in terms of model characteristics and maintenance duration. For drug mechanism studies, the model must have a sufficient duration to support subsequent intervention and drug administration experiments, which is a basic prerequisite for effective drug efficacy evaluation and mechanism exploration.

CFA is an adjuvant that enhances the immunogenicity of antigens, prolonging the residence time of injected autoantigens in the body, promoting their effective delivery to the immune system, and activating innate immune responses.[19] Therefore, it is often used as the preferred adjuvant for inducing autoimmune diseases in experimental animals, such as autoimmune encephalomyelitis (EAE)[20] and rheumatoid arthritis (RA).[21] In studies on animal models of plasma cell mastitis (PCM), Yu et al[22] employed CFA to facilitate the establishment of a PCM mouse model. Its mechanism lies in CFA's ability to serve as an antigen reservoir, continuously stimulating local inflammatory responses and granuloma formation while inducing lymphocyte proliferation and differentiation. Meanwhile, research has shown that breast tissue injected with complete Freund's adjuvant alone can produce neutrophil and lymphocyte infiltration, but no plasma cell or plasma cell-like mastitis changes were observed. The study by Zuo et al[14] also demonstrated that complete Freund's adjuvant promotes inflammation formation, but its use alone cannot induce the establishment of a GM lesion model. This suggests that the specific source of pathological features in the animal model is the tissue homogenate itself, rather than CFA. Therefore, we chose to establish and optimize the model using a combination of human GM tissue homogenate and CFA injection. Considering the homogenate as the "cargo" and CFA as the "warehouse" storing the homogenate antigen, active ingredients are slowly delivered locally to the breast to maintain moderate immune stimulation, thereby forming a chronic inflammatory response. This study confirms that the optimized tissue homogenate-CFA injection method successfully induces a GM rat model with pathological changes and characteristics closer to human GM, and the model can be maintained for at least 4 weeks. The results showed that typical pathological changes, such as residual granuloma structure, scattered chronic inflammatory cells, and a large number of scattered lipid vacuoles, could still be observed 28 days after modeling.

We evaluated the choice of experimental animals. In studies on non-lactating mastitis, the commonly used experimental animals are mainly Wistar rats and SD rats. We decided to use sexually mature female SD rats with an initial body weight of approximately 200g at 6–7 weeks of age. At this stage, the rats' mammary glands are fully developed and have reproductive capabilities, allowing them to simulate the breast state of women of reproductive age (the predisposing stage of this disease). Simultaneously, their immune system is mature, enabling a better simulation of human autoimmune responses. Studies have shown that in CFA-induced RA models,[23] SD rats exhibit higher disease susceptibility and more persistent and consistent disease characteristics compared to Wistar rats. In the EAE model, Zhu et al[24] found that although the EAE induction rate was not significantly different between SD and Wistar rats, the incubation period was longer in SD rats, and the neurological symptoms and overall central inflammatory changes were more severe than in Wistar rats. Additionally, in osteoarthritis models, SD rats show more severe osteoporosis, osteophyte formation, and local joint inflammation than Wistar rats.[25] In a uric acid sodium crystal-induced gouty arthritis model, SD rats exhibited a strong inflammatory response in the joints, with more pronounced redness and swelling compared to Wistar rats, and a higher rate of change in the inflammatory factor IL-1β.[26] Overall, SD rats have a stronger susceptibility to autoimmune and inflammatory diseases, and they are relatively inexpensive, easily accessible, and have a low mortality rate. This provides a reliable basis for our selection of SD rats as the GM modeling platform.

In this study, we determined the optimal modeling injection dose to be 0.4mL. In previous GM animal model studies, 0.2mL was the most commonly used injection volume. It's worth noting that although the modeled animals could induce typical pathological changes such as granulomatous nodules and lipid vacuoles, the duration was insufficient, causing the model to disappear quickly.[14] Therefore, we used this dose as a benchmark, incremented it in multiples, and set low, medium, and high dose groups. The tissue volume to saline volume ratio was changed from 1:3 to 1:1, increasing the antigen concentration. The results showed that at 14 days of modeling, the middle-dose group (0.4mL) exhibited more pronounced local inflammatory changes than the low-dose group (0.2mL) and more typical pathological features than the high-dose group (0.8mL). Further modeling with a 0.4mL injection revealed that the model group's rat breasts exhibited a pattern of change from lump to abscess to ulceration to sinus or fistula formation, which is consistent with the common

disease progression of clinical GM patients from the lump stage to the abscess stage to the ulceration stage.[27] Additionally, regarding the choice of modeling site, we decided to model only on the left third breast of the rats. Normally, the third pair of breasts in SD rats are located at the thoracoabdominal junction, which can simulate the breast position of normal human females. Clinically, most GM cases usually occur on one side, and bilateral cases are rare.[28] We believe that modeling only one breast is beneficial for observing the state of the modeled breast and comparing its appearance with the contralateral breast of the same pair. Moreover, it avoids mutual interference between breast masses caused by multiple modeling sites. Furthermore, we optimized some operational details. For instance, we used a 0.1mL syringe needle with a 2.5mL syringe tip. The appropriately sized needle prevents the injection material from clogging and affecting the operation, while avoiding additional damage to local tissues caused by an oversized needle. We also summarized the experience of rotating the needle during withdrawal, which effectively prevents the injection material from leaking out.

Previous studies have suggested that GM is a disease associated with an imbalance in immune response, often accompanied by an increase in various inflammatory factors.[29] Our research findings support this observation. In this study, we found that the levels of IL-2, IL-1β, TNF-α, and IFN-γ in the serum and mammary glands of rats after modeling were higher than those in normal rats, indicating that GM not only presents as a local mammary gland inflammation but also involves systemic immune activation. Compared to day 7 of modeling, most inflammatory factors further increased at day 14 or 21, which may suggest that immune cells in the body are continuously activated at this time, exacerbating the inflammatory response and promoting the rupture and pus formation of the lump. Among them, serum IL-2 and IL-1β showed a significant increase at day 14 of modeling, while the peak of TNF-α appeared at day 21. We speculate that different inflammatory factors play staged roles in the inflammatory process of GM. IL-2 is a pleiotropic cytokine produced after antigen activation that plays a key role in the immune response. It can initiate the expansion of Th1 cells.[30] Activated Th1 cells secrete IFN-γ, which further enhances Th1 differentiation through a positive feedback loop.[31] Activated Th1 cells can activate macrophages and secrete IL-1β and TNF-α. Studies have shown that IL-1β and TNF-α are released in the early stages of inflammation and continuously secreted, which can promote the release of other inflammatory mediators and rapidly exacerbate the inflammatory response.[32] Thus, these inflammatory factors exhibit a pattern of "early activation - mid-stage amplification - late-stage maintenance" in the GM model, and promote the progression of immune inflammation through mutual interactions. This is corroborated by the chronic inflammatory changes observed in the histological morphology of the model rats, characterized by continuous infiltration of immune cells such as lymphocytes and plasma cells.QRT-PCR results showed that the mRNA expression trends of various inflammatory factors in the mammary gland were basically consistent with those in the serum. Among them, TNF-α maintained a relatively high level on day 28, suggesting that the local inflammation of mammary gland tissue has a more persistent activation state than the systemic response. Some studies have pointed out that TNF-α is crucial for the formation of granulomas, which is closely related to its mediation of T-cell chemotaxis.[33,34] Interestingly, although the serum inflammatory factor levels in the normal group remained generally stable at different time points, the expression of IL-1β and TNF-α in the tissues also showed a slight increase at 21 and 28 days ($P < 0.01$ or $P < 0.05$). We consider that this may be related to physiological inflammation regulation induced by the endocrine cycle or environmental stress of the experimental animals. Nevertheless, their expression levels were still much lower than those in the model group during the same period, indicating that this model has good inflammation specificity.

Conclusion

We have optimized the animal modeling method for GM, determining the optimal injection volume for modeling as 0.4mL. Through comprehensive evaluations including appearance, auxiliary examinations, histopathology, and inflammatory factor expression, we have established a more durable GM rat model that closely resembles human clinical manifestations and pathological changes. This modeling approach has demonstrated consistent and stable results across multiple experiments. However, similar to previous animal models, this model also has limitations. For instance, it cannot simulate common GM complications such as interstitial pneumonia, erythema nodosum, and articular inflammation. Due to the complexity of the homogenate components, it remains unclear which specific active components contribute to the GM manifestations in the model animals. Perhaps this uncertainty is a tangible reflection of the model's alignment with the complex etiology of the

disease. In future studies, we will utilize this model to further explore the mechanisms underlying GM and potential therapeutic agents, particularly focusing on the immune-related mechanisms in GM.

Data Sharing Statement

The datasets used or analyzed during the current study are available from the corresponding author upon reasonable request.

Acknowledgments

We sincerely appreciate the efforts of all authors who contributed to this study.

Author Contributions

All authors made a significant contribution to the work reported, whether that is in the conception, study design, execution, acquisition of data, analysis and interpretation, or in all these areas; took part in drafting, revising or critically reviewing the article; gave final approval of the version to be published; have agreed on the journal to which the article has been submitted; and agree to be accountable for all aspects of the work.

Funding

The work received financial assistance from the National Natural Science Foundation of China (82474519), the Project of Hunan Provincial Department of Education (23A0291).

Disclosure

The authors have no conflicts of interest in this work.

References

1. Kessler E, Wolloch Y. Granulomatous mastitis: a lesion clinically simulating carcinoma. *Am J Clin Pathol*. 1972;58(6):642–646. doi:10.1093/ajcp/58.6.642
2. Musleh A, Shrateh ON, Ishtaya N, et al. A single center experience with a rare clinical entity of idiopathic granulomatous mastitis: case series and review of the literature. *Int J Surg Case Rep*. 2024;115:109232. doi:10.1016/j.ijscr.2024.109232
3. Yuan Q, Xiao S, Farouk O, et al. Management of granulomatous lobular mastitis: an international multidisciplinary consensus (2021 edition). *Mil Med Res*. 2022;9(1):20. doi:10.1186/s40779-022-00380-5
4. Hua C, Li F, Shi Y, et al. Long-term outcomes of traditional Chinese medicine in the treatment of granulomatous lobular mastitis: a two-year follow-up study on recurrence and new occurrence rates with analysis of risk factors. *J Inflamm Res*. 2024;17:7389–7399. doi:10.2147/JIR.S485589
5. Tian C, Wang H, Liu Z, et al. Characteristics and management of granulomatous lobular mastitis associated with antipsychotics-induced hyperprolactinemia. *Breastfeed Med*. 2022;17(7):599–604. doi:10.1089/bfm.2021.0341
6. Tasci HI, Turk E, Erinanc OH, et al. Factors affecting recurrence of idiopathic granulomatous mastitis. *J Coll Physicians Surg Pak*. 2022;32(2):161–165.
7. Liu R, Luo Z, Dai C, et al. Corynebacterium parakroppenstedtii secretes a novel glycolipid to promote the development of granulomatous lobular mastitis. *Signal Transduct Target Ther*. 2024;9(1):292. doi:10.1038/s41392-024-01984-0
8. Gan Q, Ding Y, Wu Y, et al. Infections due to Corynebacterium kroppenstedtii with focus on granulomatous lobular mastitis for tissue specificity, pathogenesis, bacteriologic workup, and treatment. *Arch Pathol Lab Med*. 2025. doi:10.5858/arpa.2024-0365-OA
9. Xie L, Feng J, Gao Q, et al. The autoimmune profiles in the etiopathogenesis of granulomatous lobular mastitis. *Immunobiology*. 2025;230(2):152878. doi:10.1016/j.imbio.2025.152878
10. Seyidli C, Aydogdu YF, Buyukkasap C, et al. The role of tissue IgG4 levels in steroid therapy in patients with idiopathic granulomatous mastitis. *Clin Exp Med*. 2024;24(1):173. doi:10.1007/s10238-024-01444-7
11. Wang X, He X, Liu J, et al. Immune pathogenesis of idiopathic granulomatous mastitis: from etiology toward therapeutic approaches. *Front Immunol*. 2024;15:1295759. doi:10.3389/fimmu.2024.1295759
12. Zhou Y, Liu L, Liu J, et al. Mechanism of Chaihu Qinggantang in Intervening NLRP3/IL-1β pathway to treat granulomatous lobular mastitis in rat mode. *Chin J Exp Traditional Med Formulae*. 2022;28(15):1–7.
13. Manciocco A, Chiarotti F, Vitale A, et al. The application of Russell and Burch 3R principle in rodent models of neurodegenerative disease: the case of Parkinson's disease. *Neurosci Biobehav Rev*. 2009;33(1):18–32. doi:10.1016/j.neubiorev.2008.08.002
14. Zuo X, Shi X, Liu J, et al. Establishment of a rat model of granulomatous lobular mastitis. *Laboratory Animals Comparative Med*. 2021;41(04):299–304.
15. Ma L, Chen H, Wu J. The establishment of granulomatous mastitis rat model. *J Tissue Eng Reconstructive Surg*. 2024;20(02):184–189.
16. Liu X, Su Q, Li J, et al. Establishment of a rat model of idiopathic granulomatous mastitis and investigation of IL-6 and IL-10 immune imbalance. *Med Animal Prevention Control*. 2022;38(09):825–829+920.

17. Wang M, Zeng Y, Liu M, et al. Rat model of cystic neutrophilic granulomatous mastitis by Corynebacterium kroppenstedtii. *J Inflamm Res*. 2025;18:1887–1898. doi:10.2147/JIR.S500310
18. Chinese expert consensus on the pathological diagnosis of granulomatous lobular mastitis (2024 version). *Zhonghua Bing Li Xue Za Zhi*. 2024;53(10):996–1004. doi:10.3760/cma.j.cn112151-20240612-00382
19. Billiau A, Matthys P. Modes of action of Freund's adjuvants in experimental models of autoimmune diseases. *J Leukoc Biol*. 2001;70(6):849–860. doi:10.1189/jlb.70.6.849
20. Lazarevic M, Stanisavljevic S, Nikolovski N, et al. Complete Freund's adjuvant as a confounding factor in multiple sclerosis research. *Front Immunol*. 2024;15:1353865. doi:10.3389/fimmu.2024.1353865
21. Zhong Y, Zhang L, Lu W, et al. Moxibustion regulates the polarization of macrophages through the IL-4/STAT6 pathway in rheumatoid arthritis. *Cytokine*. 2022;152:155835. doi:10.1016/j.cyto.2022.155835
22. Yu J, Bao S, Yu S, et al. Mouse model of plasma cell mastitis. *J Transl Med*. 2012;1(Suppl 1):S11. doi:10.1186/1479-5876-10-S1-S11
23. De S, Kundu S, Chatterjee M. Generation of a robust model for inducing autoimmune arthritis in Sprague Dawley rats. *J Pharmacol Toxicol Methods*. 2020;102:106659. doi:10.1016/j.vascn.2019.106659
24. Zhu Y, Zheng R, Li X, et al. Comparison of the pathogenesis of experimental autoimmune encephalomyelitis in Sprague-Dawley and Wistar rats. *Acta Laboratorium Animalis Scientia Sinica*. 2009;17(03):166–171+251.
25. Warmink K, Rios JL, van Valkengoed DR, et al. Sprague Dawley rats show more severe bone loss, osteophytosis and inflammation compared to Wistar han rats in a high-fat, high-sucrose diet model of joint damage. *Int J Mol Sci*. 2022;23(7):3725. doi:10.3390/ijms23073725
26. Zhu J, Wu P. Evaluation on the preparation of two different strains of rats gouty arthritis model. *J Med Res Combat Trauma Care*. 2014;27(05):478–481.
27. Liu X, Chen Q. Expert consensus on Chinese medicine diagnosis and treatment of granulomatous lobular mastitis (2021 edition). *Chin J Surg Integrated Traditional Western Med*. 2022;28(05):597–602.
28. Ge T, Sun P, Feng X, et al. Clinical features and risk factors of bilateral granulomatous lobular mastitis. *Medicine*. 2024;103(17):e37854. doi:10.1097/MD.0000000000037854
29. Lou Y, Xu H, Lu Z, et al. Immune regulation: a new strategy for traditional Chinese medicine-based treatment of granulomatous lobular mastitis. *Front Immunol*. 2024;15:1494155. doi:10.3389/fimmu.2024.1494155
30. Boyman O, Sprent J. The role of interleukin-2 during homeostasis and activation of the immune system. *Nat Rev Immunol*. 2012;12(3):180–190. doi:10.1038/nri3156
31. Saravia J, Chapman NM, Chi H. Helper T cell differentiation. *Cell Mol Immunol*. 2019;16(7):634–643. doi:10.1038/s41423-019-0220-6
32. Wang Y, Che M, Xin J, et al. The role of IL-1beta and TNF-alpha in intervertebral disc degeneration. *Biomed Pharmacother*. 2020;131:110660. doi:10.1016/j.biopha.2020.110660
33. Silva DAAD, Silva MVD, Barros CCO, et al. TNF-alpha blockade impairs in vitro tuberculous granuloma formation and down modulate Th1, Th17 and Treg cytokines. *PLoS One*. 2018;13(3):e0194430. doi:10.1371/journal.pone.0194430
34. Amber KT, Bloom R, Mrowietz U, et al. TNF -α: a treatment target or cause of sarcoidosis? *J Eur Acad Dermatol Venereol*. 2015;29(11):2104–2111. doi:10.1111/jdv.13246